A NEW ROUTE FOR WATER INTRODUCTION IN A MICRO GAS TURBINE CYCLE

W. De Paepe[a,*], F. Contino[a], F. Delattin[a], S. Bram[a,b] and J. De Ruyck[a]
[a] Vrije Universiteit Brussel, Pleinlaan 2, 1050, Brussels, Belgium
[b] Erasmushogeschool, Nijverheidskaai 170, 1070, Brussels, Belgium
*corresponding author: wdepaepe@vub.ac.be

ABSTRACT

Micro gas turbines (mGT) offer some advantages for small scale (up to 500 kW_e) Combined Heat and Power (CHP) production compared to Internal Combustion Engines (ICE) due to their low vibration level, cleaner exhaust and lower maintenance cost. The major drawback is the lower electric efficiency, which makes mGTs less attractive for applications with a non-continuous demand for heat. Therefore, a reduction in heat demand will generally lead to a forced shut down of the unit, which makes the mGT less competitive compared to the ICE.

Water injection in the compressor exhaust is considered as a possible route to improve the electrical efficiency of the mGT. To determine the optimal cycle settings for water injection, we have performed simulations using a two-step method. In a first step, the thermodynamic limit for the water injection is sought using a black box method. In a second step, the cycle layout is designed by means of composite curve theory.

This paper summarizes the results of two case studies. In the first case, the black box is considered adiabatic and no fixed stack temperature is imposed (thus allowing condensation of the exhaust gasses). One of the major concerns when injecting water is the water consumption, which can be compensated in some cases through condensation and recycling of the condensate. Therefore, in the second case, the cycle is made self-sufficient with water. In this case, the black box is no longer considered adiabatic and heat exchange with the environment is allowed for condensation of the flue gasses.

Simulations showed that lowering the stack temperature to 53°C results in an injection of 17 %wt of water and an increase in electric efficiency of 9% absolute. Results of simulations of the second case indicate that the stack temperature needs to be lowered under 30°C in order to make the cycle self-sufficient with water.

Keywords: micro gas turbine, water injection, black box method, composite curve theory, exergy.

INTRODUCTION

Micro gas turbines (mGT) offer a number of advantages compared to Internal Combustion Engines (ICE) for small-scale (up to 500 kW_e) power production, for example, a small number of moving parts, compact size and light weight and opportunities for better energy efficiency, lower emissions and lower electricity costs [1]. Particularly for the small-scale Combined Heat and Power (CHP), mGTs offer great potential [2-5]. The major drawback is the lower electric efficiency. A lower heat demand mostly leads to a forced shutdown of the engine, due to the low electric efficiency because producing only electricity with the mGT is more expensive than taking the necessary power from the grid. This forced shutdown reduces the total amount of yearly running hours, making the investment less attractive [6].

A first way to improve the performance of the mGT system is by finding the optimal nominal power and number of mGTs necessary in the small-scale CHP system [7] and by optimizing the operational planning [8].

A second way to improve the overall performance of an mGT CHP unit is by improving the electric efficiency of the mGT. Increasing the electric efficiency will make the mGT more competitive against the ICE engine.

Electric efficiency can be improved by increasing the efficiency of the components of the mGT. According to McDonald, the two parameters that have potential for efficiency increase are increased Turbine Inlet Temperature (TIT) and higher recuperator effectiveness [9]. Since cooling of the small radial flow turbine is difficult, the TIT can only be increased if thermal resistant – ceramic – materials are introduced in the mGT. The use of these ceramic materials allow for a higher TIT, resulting in considerable energy savings [10, 11]. Campanari et al. showed that the high

electric efficiency levels achievable with future advanced ceramic mGTs would improve dramatically the economic competitiveness of the application, as well as the primary energy savings and environmental benefits [12]. By using a heat resistant coating technology, Kim and Lee were able to increase the TIT of their home made mGT by 100°C, resulting in 20% more power output and 6% absolute increase in electric efficiency [13]. Increasing the recuperator efficiency is very straight forward, but will however result in a dramatically increase in recuperator size, weight and cost [9]. Pressure drop over the recuperator should be limited, since a 1% pressure loss increase will decrease the turbine efficiency by 0.33% [14]. A higher TIT will also require superalloys for the recuperator design. McDonald proposes a basic concept for better heat exchanger design [15].

Another way to improve the electric efficiency of the mGT is by introducing water (vapour/liquid) in the cycle. Water injection is considered a successful way to increase electric efficiency of Gas Turbine (GT) cycles [16]. In periods with a low heat demand, the lost thermal power can be recovered by introducing auto-raised steam/heated water inside the mGT cycle, resulting in a more profitable investment [6]. The beneficial effect of steam/water introduction in an mGT on its performance has already been studied several times [17-23]. Lee et al. showed by means of simulations the beneficial effect of steam injection on the performance of a recuperated mGT cycle [17]. Dodo et al. equipped a 150 kW_e mGT with a Humid Air Turbine (HAT) and Water Atomizing inlet air Cooling (WAC) [18]. Experiments showed stable runs at 32% electric efficiency and reduced NO_x exhaust. Mochizuki et al. performed steam injections experiments on a Capstone C60 mGT. At 60 kW_e and injection up to 6 wt% steam/air ratio, thermal efficiency could be improved by 3 to 4% [19]. Parente et al. studied the thermodynamic and the thermo-economic performance of a micro Humid Air Turbine (mHAT) [20, 21]. Delattin et al. simulated [6] and De Paepe et al. validated the effects of steam injection on a Turbec T100 mGT [23]. Recently, the authors of this paper presented a study on the performance of a T100 mGT when injecting water. By means of a two-step method – the first step being the determination of the thermodynamic limit by using a black box method, and the second step, using composite curve theory to design the heat exchanger network layout – the potential for water injection in an mGT was studied [24].

In this paper, the results of two case studies concerning the water injection in an mGT are presented. In the first case [Case Study 1 (CS1)], the black box is considered adiabatic and no fixed stack temperature is imposed (thus allowing condensation of the exhaust gasses). Since water consumption is a major issue for mixed air/water GTs, in the second case study [Case Study 2 (CS2)], the cycle is made self-sufficient with water. In this case, the black box is no longer considered adiabatic and heat exchange with the environment is necessary to condense the flue gasses.

APPROACH

The Turbec T100 microturbine CHP system is a typical recuperated mGT system (Figure 1). The inlet air enters the compressor (1), where it is compressed. The compressed air is preheated in the air recuperator by the hot flue gasses (2). In order to obtain the best performance, the compressed air is heated until maximal TIT (950°C) by burning natural gas in the combustion chamber (3). The hot gasses will expand over the turbine (4), which is connected to a high-speed generator. After preheating the compressed air, the excess heat, available in the flue gasses is used to heat water for heating purpose (5). A brief summary of the mGT performance is given in Table 1.

Table 1: General specifications of the T100 mGT.

Electric power	100 kW_e
Thermal power	167 kW_{th}
Electric efficiency	30%
Thermal efficiency	50%
Nominal shaft speed	70 000 rpm

The T100 mGT produces a constant electric power output (user defined between 60 and 100 kW_e). The produced thermal power can be controlled by routing part of the exhaust gasses directly to the stack and thus bypassing the

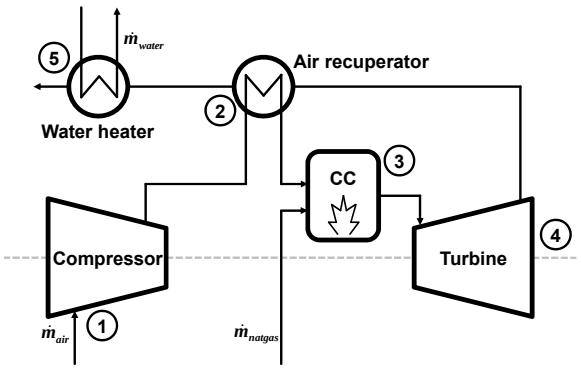

Figure 1: The compressed air (1) is preheated by the flue gasses in the recuperator (2) and heated in the combustion chamber (3) by burning natural gas. Expanding the hot gasses over the turbine provides the power (4). Finally, hot flue gasses are used to heat water for domestic heating purpose (5).

water heater. This will however lower the thermal efficiency of the mGT. The compressor and turbine of the T100 work at a variable shaft speed, which results in variable mass flow rate and pressure ratio. The controller of the T100 will adjust the shaft speed in order to keep the power output constant. Next to the shaft speed, the fuel flow is also controlled in order to maintain TIT at is maximal value.

The current paper summarizes the results of two series of water injection simulations, performed on the Turbec T100 mGT. A two-step procedure, developed by Bram and De Ruyck for the design of mixed air/water GTs, has been used [25, 26]. The potential of this procedure has been shown by the development of a new humidified GT, without using a saturation tower, the REgenerative EVAPoration cycle (REVAP®) [27, 28]. In this procedure, the thermodynamic potential of water injection is first studied, using an adiabatic black box method. In a second step, the final cycle layout is designed, using composite curve theory.

METHOD

All simulations, presented in this paper, are performed using Aspen® plus simulation engine (version 2006.5). Simulations were performed at constant nominal power of the T100 mGT (100 kW_e). In the following subsections, the modelling of the T100 mGT in Aspen® will be discussed. Next to the modelling of the mGT components, the black box simulation method and exergy analysis are discussed. Finally, additional information about the composite curve theory, used to design the heat exchanger network, is given.

mGT components modelling

For the modelling of the mGT in the Aspen® plus simulation engine, an adapted version of previous developed models of the dry and wet mGT [6] are used. These models were validated in [23]. The existing controller of the T100 mGT is implemented in the Aspen® models. The controller keeps the electric power and TIT constant by adapting compressor shaft speed and natural gas flow. In the Aspen® models, constant electric power and TIT are set as design specifications. By varying shaft speed and natural gas flow, the Aspen® solver can converge to a solution, respecting the design specifications.

For the modelling of the compressor, generic compressor maps were used. When water is injected in the cycle, the total mass flow rate through the turbine will increase, resulting in a higher turbine/electric power. To keep the produced electric power constant, rotation speed is decreased, resulting in a lower compressor mass flow rate (off-design). Since it is the goal of this paper to find the limit for water injection in the mGT, the operation point of the compressor will move away from the optimal dry operating point, resulting in a lower isentropic compressor efficiency. For this reason, areas of constant compressor efficiency were implemented in the Aspen® compressor maps.

In the model used for the turbine, the turbine is assumed to be chocked. Mathematically this is expressed as:

$$\frac{\dot{m}_{turb}\sqrt{TIT}}{PIT} = A\sqrt{\frac{k_{turb}}{R}\left(\frac{2}{k_{turb}+1}\right)^{\frac{k_{turb}+1}{k_{turb}-1}}} \qquad (1)$$

Due to the injection of water, the heat capacity ratio (k_{turb}) in Eq. (1) will change (0.1% per injected water fraction), resulting in a different chocking value. Next to the chocking condition, the isentropic efficiency of the turbine will also change due to water injection. Dry turbine efficiency is equal to 0.85 and is compensated using

$$\frac{\eta_{is}}{\eta'_{is}} = \frac{k'-1}{k-1}\sqrt{\frac{k'+1}{k+1}\frac{1-1/\beta^{\gamma'}}{1-1/\beta^{\gamma}}} \text{ [20].} \qquad (2)$$

In Eq. (2), the apex (') refers to the property at standard air composition. γ is defined as $(k-1)/k$. Both corrections were added to the simulation model.

The heat exchangers were modelled with generic heat exchanger models. Pressure loss over the hot side of the heat exchange network was set to 3% of the total pressure, for the cold side, a pressure drop of 40 mbar was imposed. These losses correspond to the actual losses in the dry cycle of the T100. The losses are design conditions, which are a trade-off between the cost of the heat exchanger, which increase if the heat exchangers becomes larger, and the pressure loss, which has a huge effect on turbine performance [14].

Black box analysis

For the simulations performed in the first step of the two-step method, all heat exchangers in the mGT layout from Figure 1 were removed and replaced by a black box. For the first case study (CS1), an adiabatic black box was used, for the second case study (CS2), heat exchange with the environment (heat sink) was allowed, since the flue gasses needed to be cooled in order to make the cycle self-sufficient with water. In Aspen®, a straightforward implementation of a black box does not exist. Bram and De Ruyck [26] proposed an alternative, by generating a network of generic heaters and coolers, that would act as a black box system. A modified

version of the network, proposed in [26] and used in [24], is used for the simulations performed for this paper. The T100 has only one compressor stage, so there is no intercooling, which reduces the amount of heaters and coolers in the network.

For CS1, the network design as depicted in Figure 2 has been used. For the first case study, the water is first injected in the compressed air. Before entering the combustion chamber, the air/water mixture is preheated in the HEATER. The flue gasses coming from the turbine are then cooled in COOLER before they are ejected through the stack. Expressing the conservation of the energy over the black box, a correlation between the thermal power of the heater and cooler can be expressed as:

$$\dot{Q}_{COOLER} + \dot{Q}_{HEATER} = 0\ . \qquad (3)$$

In the black box, there are three parameters that can be controlled, but only two degrees of freedom, since the compressor outlet mass flow rate, pressure and temperature and the Turbine Outlet Temperature (TOT) are controlled by the mGT control system (power output and TIT control). If the temperature difference on the hot side of the black box is imposed (hot pinch), together with the stack temperature, and taking into account the energy balance in Eq. (3), the amount of water that must be injected is set.

The major disadvantage of mixed air/water GTs is the large water consumption [29]. By introducing a condenser in the cycle, it is possible to recover all the injected water [30, 31]. The goal of CS2 is to check the possibility to make the cycle self-sufficient for water. For this case study, the black box layout is slightly adjusted (additional grey parts in Figure 2). The flue gasses coming from COOLER in Figure 2 are cooled further in CONDENS to get condensation of the water present in the flue gasses. The excess heat of the CONDENS-cooler ($\dot{Q}_{CONDENS}$) is rejected to the environment. Again, three parameters can be controlled in the black box, while there are only two degrees of freedom. In this case, if we impose the hot pinch and the heat disposal to the environment, the stack temperature and the amount of circulating water are set, due to the closed loop.

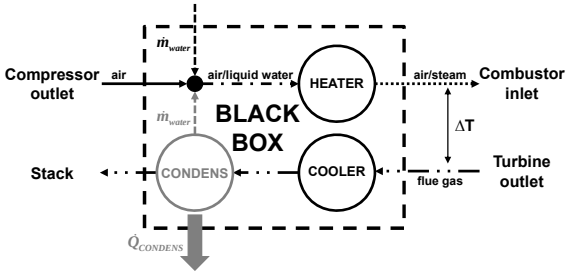

Figure 2: Black box layout used for simulations of Case Study 1 (CS1) and Case Study 2 (CS2, grey parts).

The boundary conditions used for the black box simulations of CS1 and CS2 are shown in Table 2. The stack temperature during simulations is variable. Rather than applying a specific stack temperature to the black box system, it was decided to control the amount of injected water. Simulations showed that controlling $\dot{m}_{water}$ allows Aspen® to reduce the convergence time, especially when condensation appears in the flue gasses.

Exergy analysis of the black box systems

The exergy destruction and efficiency of the black box are defined as described in [24].

Exergy efficiency is defined as the ratio between the sum of the exergy of the streams that gain exergy, and the sum of the exergy of the streams that lose exergy. For both CS1 and CS2, the exergy efficiency is thus reduced to the ratio between the exergy gain of the compressed air and the exergy loss of the flue gasses. Since the water injection system is designed to overcome the lower heat demand,

Table 2: Boundary conditions used in the black box simulations of CS1 and SC2.

Compressor	
Pressure ratio	Variable[1]
Isentropic efficiency	Variable[1]
Inlet air temperature	15°C
Turbine	
Turbine back pressure	50 mbar
Isentropic efficiency	Variable[2]
Turbine inlet temperature	950°C
Combustion chamber	
Combustor pressure loss	5%
Heat recovery system	
Hot side pressure loss	3%
Cold side pressure loss	40 mbar
Water injection pressure loss	0.5%
Hot side temperature difference	50°C
Stack temperature	Variable[3]
Feed water inlet temperature	15°C
Fuel (methane)	
Fuel temperature	30°C
Fuel pressure	6 bar
LHV	50 MJ/kg
General	
Produced electrical power	100 kW_e

[1]For the simulations, generic compressor maps were used.

[2]The isentropic efficiency depends on the water content of the working fluid, but TIT is constant.

[3]The final stack temperature depends on the amount of water that needs to be injected.

the condensation heat $\dot{Q}_{CONDENS}$ is seen as a loss and is therefore not introduced in the exergy balance. For the calculation of the exergy of the different streams, an in-house Fortran procedure has been used [26].

For each amount of injected water, exergy destruction and efficiency were calculated. In literature, values of a global exergy destruction of minimal 5% and a black box exergy efficiency as high as 93 % are used as limits for the heat transfer systems [32]. Crossing these limits will lead to unrealistic designs, too difficult to realize with real heat exchangers.

Heat exchanger design

For the final design of the heat exchanger network, based upon results of black box analysis, composite curve theory was used [33]. For the composite curves, a minimum pinch of 10°C was set as design condition.

For all simulations, the same boundary conditions as given in Table 2 and used for the black box simulations were used. For the heat exchangers, an additional condition was used: 10°C minimal temperature difference between the hot exhaust and cold inlet. Furthermore, generic heat exchanger models were used, since the actual design of the heat exchangers is beyond the scope of this paper.

RESULTS

Before discussing the results of the case studies, two possible problems with water injection are discussed: surge margin reduction and combustion stability.

Surge margin reduction and combustion stability

The Turbec T100 mGT works at constant power. As mentioned before, the mGT controller will keep the power constant by decreasing the compressor mass flow rate by reducing the shaft speed. Since water will be injected after the compressor, but before the turbine, there is an unbalance in mass flow rate, resulting in a higher turbine power and additional produced electrical power. To keep the power output constant, the shaft speed is reduced. This shaft speed reduction result into a decreasing pressure ratio and air mass flow rate in the compressor. The shaft speed reduction will shift the compressor operation point to the surge limit. According to Walsh and Fletcher, a minimal surge margin of 15-20% is necessary for low-pressure compressors in power generation applications [34].

Due to the injection of water, some problems with combustion stability may arise. The combustion instabilities can lead to reduced combustion efficiency and an increasing emission of carbon monoxide and unburned hydrocarbons [16]. The addition of water has however, a positive effect on NO_x exhaust [35-37]. According to Hermann et al., the limit for combustion is 33 wt% of water in the gasses; because combustion become unstable at this point due to the CO levels [37].

Black box

For both CS1 and CS2, water and compressed air are mixed before entering the HEATER (Figure 2). Depending on the amount of water, the mixture entering the HEATER is either humidified air, fully saturated air or saturated air that still contains liquid water droplets. All remaining droplets however will evaporated in the HEATER.

With increasing injected water, the stack temperature in CS1 decreases linearly (Figure 3). The more water is injected, the more heat needs to be exchanged between the flue gasses and the wet compressed air in order to reach a combustor inlet temperature such that the hot pinch temperature is 50°C. The stack temperature reduction continues until 53°C is reached. At this point, the water inside the flue gasses starts to condensate, resulting in an extra release of heat. The total amount of water condensed is also shown in Figure 3. For this reason, it was decided to use the injected water mass flow rate as variable in the black box calculations and to calculate the stack temperature, which allowed simulating beyond the point of condensations. If a stack temperature was set to 53°C, no convergence in Aspen® was reached, since there are multiple solutions.

The stack temperature in CS2 slightly increases with increasing water mass flow rate (from 29°C at 0.005 kg/s to 32°C at 0.09°C) (Figure 3). The increasing stack temperature is a result of the decreasing air mass flow. The higher the water injection mass flow rate, the more the mGT controller will reduce the rotation speed and thus

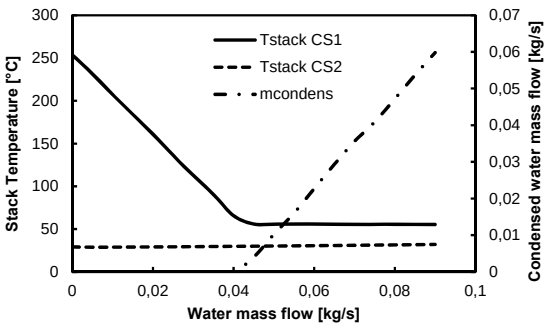

Figure 3: Stack temperature and condensed water mass flow rate as function of the injected water mass flow rate for Case Study 1 (CS1) and Case Study 2 (CS2).

the air mass flow rate. The lower the air mass flow, the less water can be evaporated in the saturated air, which results in a higher stack temperature when all necessary water is condensed. The temperature rise is however slightly slowed down since less natural gas is burned. The amount of condensed water in CS2 is not added to Figure 3, since it was the goal to make the cycle self-sufficient for water, so the total amount of condensed water corresponds to the amount of injected water.

Simulations of CS1 and CS2 were stopped at an injection of 0.09 kg/s of water for both case studies (Figure 3). At this point, the compressor had reached his surge limit (Figure 4). The impact of the water injection on the compressor performance are shown on Figure 4. As mentioned before, the operating point shifts towards the surge margin. Surge margin is reached when 0.09 kg/s of water is injected in the cycle, according to a water fraction of 17 wt%, which is still below the limit set by Hermann et al. for combustion stability [37]. In order to reach this 0.09 kg/s of water injection, compressor needs to be redesigned in order to obtain a sufficient surge margin of 15-20% [37].

For all applied water mass flow rates, the exergy destruction and efficiency are below the limits from literature [32] (Figure 5). For increasing injected water mass flow rates, the exergy efficiency of the black box from CS1, decreases first, while destruction increases. Afterwards, exergy destruction starts to decrease while exergy efficiency increases again. Exergy efficiency of CS2 increases with increasing water mass flow, while exergy destruction decreases. The higher the amount of injected water, the more energy is recuperated in the HEATER-COOLER system and less is lost in the cooling process to condensate the flue gasses. This explains the increasing efficiency and decreasing destruction. One can also see that exergy efficiency of the black box is lower than the exergy efficiency of the black box of

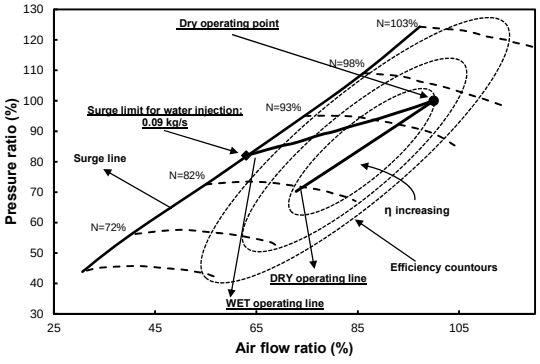

Figure 4: Compressor map showing the shift of the wet operating point towards the surge limit.

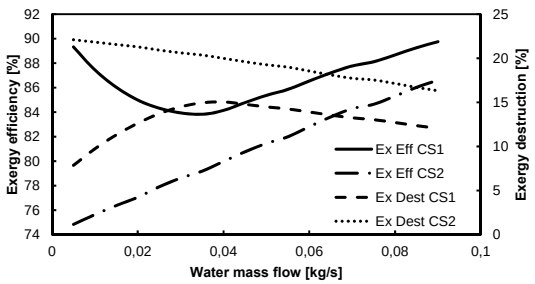

Figure 5: Exergy efficiency and destruction remain below the limit from literature for all different amounts of injected water.

CS1, which is due to the lower stack temperatures in CS2 (see Figure 3). Flue gasses are cooled to get condensation of the water; however, the exergy of this cooling process is not used, resulting in an extra loss, explaining the lower exergy efficiency.

The behaviour of exergy efficiency and destruction in CS1 can be explained by looking to the exergy fluxes entering and leaving the black box, shown in Figure 6. The exergy flow of the feed water from CS1 is not shown on Figure 5, since the water is introduced in the black box in its dead state (15°C, 1bar, liquid phase) and has therefore no exergy.

The different behaviour of the different exergy flows from Figure 6 can be explained as follows:

- With increasing water injection, the exergy flow through the turbine exhaust increases, due to the higher water content of the flow. Because of the higher water content, the TOT is also slightly higher, since TIT is kept constant by the mGT control system. The control system however also reduces the mass flow rate, which limits the exergy flow increase.
- Exergy flow at the combustor inlet however remains more or less constant. The increasing exergy flow because of the higher temperature and water content is compensated by the lower pressure and mass flow rate, resulting from the

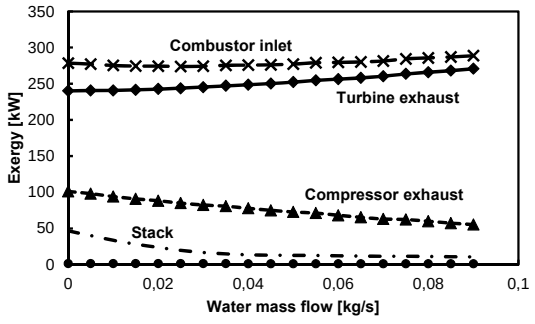

Figure 6: Different exergy flows of the black box system. Results of CS1 are shown using lines, while the corresponding results of CS2 are shown using symbols.

lower rotation speed set by the mGT controller.

- The lower pressure ratio, mass flow rate and compressor outlet temperature results in a decreasing exergy flow entering the black box from the compressor outlet.
- Since the stack temperature is gradually reduced with increasing water injection, the outgoing exergy flow through the stack is also reduced. From the injection of 0.045 kg/s of water on, the stack temperature remains constant due to the condensation of water, resulting in a stabilisation of the exergy flow.

Using previous information, exergy efficiency and destruction of CS1 of Figure 5 can be explained. The exergy flow of the stack decreases faster than the exergy flow of the compressor outlet. The exergy flow increase of the turbine exhaust is larger than the one at the combustor inlet. This results in decreasing exergy efficiency, while the exergy destruction of the black box increases. When reaching a stack temperature of 53°C, the exergy loss through the stack remains constant, resulting in increasing exergy efficiency and decreasing exergy destruction.

Comparing exergy flow of CS1 with CS2 shows only one difference. Exergy flows of the combustor inlet (cross), turbine exhaust (diamond) and compressor outlet (triangle) remain constant at the same injected water fraction, while the exergy flow of the stack (circle) is in CS2 much smaller than CS1. The stack temperature of CS2 is low compared to the stack temperature of CS1 (Figure 3). On top of this lower temperature, the amount of water vapour present in the flue gasses is much lower, due to the condensation of the necessary water, resulting in a very low exergy flow.

The electric efficiency of the mGT will increase, as expected, with increasing injected water mass flow rate (Figure 7). Although, exergy efficiency first decreases and then increases; this has no effect on the global efficiency of the mGT. The absolute efficiency rise depends on the amount of injected water. The non-linear efficiency increase is a result of the transformation of the compressor map into working lines. At an injection rate of 0.09 kg/s, the absolute efficiency rise amounts 9%. Comparing results of CS1 (line) with CS2 (diamonds) shows that there is no difference between the electric efficiency, as could be expected. In the black box system of CS2, the feed water flow is replaced by a condenser that will provide the necessary water. The heat output of this condenser is not used in the system; so finally, there is no difference between CS1 and CS2 for the mGT performance. In the actual power plant, when the losses of the auxiliaries needs to be taken into account, there will be a difference, since energy is needed for the water treatments or for the cooling of the flue gasses to get condensation (and possible also water treatment).

From the results of the electric and exergy efficiency, one can conclude that condensing the exhaust gasses needs to be accomplished with an external heat sink. None of the transferred exergy can be used in the system. The final design of the heat exchanger network is the same as for CS1, with an additional cooler on the flue gas flow to cool the flue gasses to get condensation of the required water.

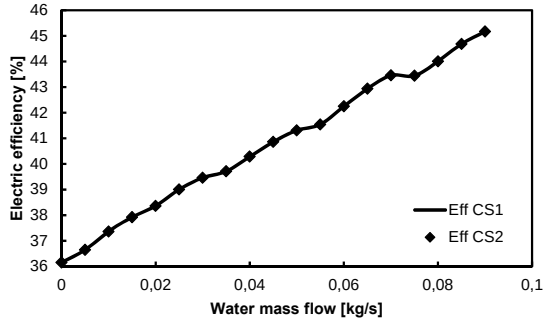

Figure 7: Electric efficiency increases with increasing injected water mass flow rate for CS1 (line) and showing good accordance with efficiency increase from CS2 (diamonds).

Heat exchanger network design

For the heat exchanger network design of CS 1, three possible layouts were simulated, as can be seen in Figure 8. A first possibility is the direct injection of the water in the compressor outlet (A), the second possibility is the injection of preheated water in the compressor outlet (B) and the final test case was the use of a saturation tower (the mHAT approach (C)).

The simulations of case (B) are divided into two subcases. In a first subcase, water was heated, but the final injection temperature remained below the boiling point. In the second subcase,

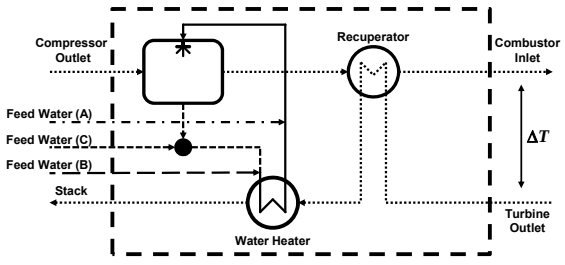

Figure 8: Heat exchanger network designs, using direct water injection (Case A), preheated water injection (Case B) and the use of a saturation tower (Case C).

liquid water was heated, boiled and the raised steam was superheated (5°C). For this subcase, where temperature at the boiling point remains constant, a different approach needs to be applied; the water heater has been split up in three parts: a water heater, a boiler and a super heater. Finally, injection of a liquid-vapour mixture was not considered.

The black box maximal water injection of 0.09 kg/s of water is never reached, because the simulated stack temperature of 53°C can never be reached (Table 3). The limitation for the stack temperature is the temperature of the working fluid mixture after water injection in Case A and C, and the low amount of water that can be heated in Case B. For direct injection, the mixing temperature of the compressed air and the liquid water is still quit high (around 63°C). The stack temperature cannot be lowered further than this mixing temperature, otherwise the composite curves will cross, which is prohibited. The same explanation as for Case A can be given for Case C, the mHAT. The temperature of the excess water leaving the saturation tower, which is rerouted to the water heater, will determine the lowest possible stack temperature. Hot flue gasses cannot be cooled below this temperature, which corresponds to the saturation temperature of the compressed air. Final composite curves are shown in Figure 9. For all composite curves, only the heat exchange inside the actual heat exchangers is considered. The mixing is not taken into account, since mixing does not require a minimal pinch. For both the direct injection and the mHAT case, the minimal pinch (10°C) can be seen at the lowest temperature of the composite curves, meaning the difference between the stack and mixing temperature, which proves that the stack temperature is determined by the mixing temperature (Figure 9 (a)).

Figure 9 (b) gives the composite curves of the indirect injection of heated liquid water (Case Water) or steam (Case Steam). For the injection of steam, the minimal pinch depends on the boiling point of the water. If the stack temperature would be lowered, hot and cold composite curve would cross, which is prohibited. For the injection of water, the minimal stack temperature depends on the amount of water injected, since one should avoid the production of steam.

Table 3: Results of heat exchanger network design, using different injection types.

	Case A	Case B		Case C
		liquid	steam	
T_{stack}	75°C	64°C	125°C	84°C
T_{mix}	65°C	67°C	173°C	75°C
$\dot{m}_{water}$	38 g/s	40 g/s	27 g/s	36 g/s
η_{el}	40.2%	40.5%	39.5%	39.9%
$\dot{Q}_{CONDENS}$	128 kW	126 kW	133 kW	130 kW
$T_{CONDENS}$	30.0°C	30.1°C	29.6°C	29.7°C

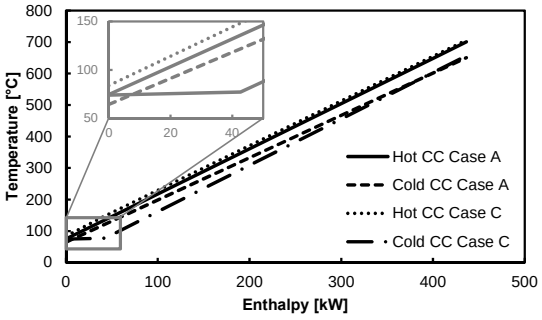

(a)

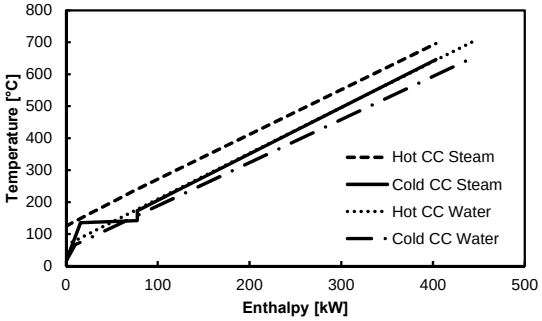

(b)

Figure 9: Composite curves of direct water injection (Case A) and the mHAT case (Case C) and the injection of heated water (Case B Water) and auto-raised steam (Case B Steam).

Even though exergy analysis of the black box showed that injection up to 0.09 kg/s of water (surge limit of the compressor) still results in a global exergy efficiency and destruction below limits that can be found in literature [32], this potential cannot fully be explored, due to local violations of the second law.

In Table 3, results of the electric efficiency simulations showed that the lower the stack temperature, the more water that can be injected, resulting in a higher electric efficiency. Injection of heated water is the most efficient way of water injection; however, differences between the different cases are rather small. Results of condensation simulations show that the lower the injected amount of water, the more the stack temperature needs to be lowered and the more heat needs to be disposed to the environment in order to make the cycle self-sufficient with water.

When the maximal amount of water is injected, by means of injection of heated water, the surge margin is reduced from 25% to 16%, which is still within the limits for power generation [34].

The water fraction is limited to 6.7 wt%, which should still allow for a stable combustion [37].

CONCLUSION

The results of a series of simulations of water injection in the compressor outlet of an mGT are presented. Water injection can increase the yearly amount of running hours of an mGT, since the electric efficiency will increase due to addition of water. To find the thermodynamic optimal of the water injection, the heat exchanger network of the mGT has been replaced by a black box system. Two case studies were applied on this system. The first study investigated the maximal potential for water injection, by lowering the stack temperature, without violation of the second law of thermodynamics. In the second case study, the cycle was made self-sufficient with water by condensing the water in the exhaust gasses; since the cost of the water consumption and treatment is a major drawback of humidified gas turbines. The final heat exchanger network was designed using composite curve theory.

Results of black box simulations indicated that lowering the stack temperature to 53°C results in an injection of 17 %wt of water and an increase in electric efficiency by 9% absolute, without a violation of the global exergy balance over the black box system. Composite curve theory and pinch analysis however showed that lowering stack temperature until 53°C is not possible. The lowest possible stack temperature, depending on the injection type is 74°C (direct injection of water), 64°C (direct injection of heated water) and 84°C (mHAT). These stack temperature respectively corresponded to an injection of 37 g/s, 40 g/s and 36 g/s of water, which resulted in absolute efficiency increases of 4.2%, 4.4% and 3.8%.

Results of the second case study indicate that the stack temperature needs to be 30°C or lower to become fully self-sufficient for water.

NOMENCLATURE

Abbreviations

CHP	Combined Heat and Power
CS1	Case Study 1
CS2	Case Study 2
GT	Gas Turbine
ICE	Internal Combustion Engines
mGT	micro Gas Turbine
REVAP	Regenerative EVAPoration
TIT	Turbine Inlet Temperature [°C]
TOT	Turbine Outlet Temperature [°C]
WAC	Water Atomizing inlet Cooling

Symbols

A	Turbine inlet cross section [m²]
β	Pressure ratio
k	Heat capacity ratio (c_p/c_v)
$\dot{m}$	Mass flow rate [kg/s]
η	Efficiency [%]
PIT	Turbine inlet pressure [Pa]
R	Gas constant [kJ/kgK]
$\dot{Q}$	Heat flux [kW]

Subscripts

CONDENS	condensor
COOLER	cooler
el	electric
HEATER	heater
is	isentropic
mix	condition of mixing point
stack	condition of stack flow
water	condition of water flow
turb	condition inside turbine

ACKNOWLEDGMENT

The research was funded by the National Fund for Scientific Research (FWO).

REFERENCES

[1] U.S. Department of Energy, Office of Energy Efficiency and Renewable Energy, Office of Power Technologies, Advanced Microturbine Systems – Program plan for fiscal years 2000 through 2006, 2000.

[2] P.A. Pilavachi, Mini- and micro-gas turbines for combined heat and power, Applied Thermal Engineering, 22 (2002) 2003 - 2014.

[3] S. Gamou, R. Yokoyama, K. Ito, Parametric Study on Economic Feasibility of Microturbine Cogeneration Systems by an Optimization Approach, Journal of Engineering for Gas Turbines and Power, 127 (2005) 389-396.

[4] J. Kaikko, J. Backman, Technical and economic performance analysis for a microturbine in combined heat and power generation, Energy, 32 (2007) 378 - 387.

[5] L. Galanti, A.F. Massardo, Micro gas turbine thermodynamic and economic analysis up to 500kWe size, Applied Energy, 88 (2011) 4795-4802.

[6] F. Delattin, S. Bram, S. Knoops, J. De Ruyck, Effects of steam injection on microturbine efficiency and performance, Energy, 33 (2008) 241-247.

[7] S. Sanaye, M.R. Ardali, Estimating the power and number of microturbines in small-scale

combined heat and power systems, Applied Energy, 86 (2009) 895-903.

[8] S. Gamou, K. Ito, R. Yokoyama, Optimal Operational Planning of Cogeneration Systems With Microturbine and Desiccant Air Conditioning Units, Journal of Engineering for Gas Turbines and Power, 127 (2005) 606-614.

[9] C.F. McDonald, Recuperator considerations for future higher efficiency microturbines, Applied Thermal Engineering, 23 (2003) 1463-1487.

[10] L. Goldstein, B. Hedman, D. Knowles, S.I. Freedman, R. Woods, T. Schweizer, Gas-Fired Distributed Energy Resource Technology Characterizations, N.R.E. Laboratory (ed.), 2003.

[11] A.F. Massardo, C.F. McDonald, T. Korakianitis, Microturbine/Fuel-Cell Coupling for High-Efficiency Electrical-Power Generation, Journal of Engineering for Gas Turbines and Power, 124 (2002) 110-116.

[12] S. Campanari, E. Macchi, Technical and Tariff Scenarios Effect on Microturbine Trigenerative Applications, Journal of Engineering for Gas Turbines and Power, 126 (2004) 581-589.

[13] M.T. Kim, S.W. Lee, Application of in situ oxidation-resistant coating technology to a home-made 100 kW class gas turbine and its performance analysis, Applied Thermal Engineering, 40 (2012) 304-310.

[14] G. Lagerstrom, M. Xie, High Performance and Cost Effective Recuperator for Micro-Gas Turbines, ASME Conference Proceedings, 2002 (2002) 1003-1007.

[15] C.F. McDonald, Low-cost compact primary surface recuperator concept for microturbines, Applied Thermal Engineering, 20 (2000) 471 - 497.

[16] M. Jonsson, J. Yan, Humidified gas turbines – a review of proposed and implemented cycles, Energy, 30 (2005) 1013-1078.

[17] J.J. Lee, M.S. Jeon, T.S. Kim, The influence of water and steam injection on the performance of a recuperated cycle microturbine for combined heat and power application, Applied Energy, 87 (2010) 1307 - 1316.

[18] S. Dodo, S. Nakano, T. Inoue, M. Ichinose, M. Yagi, K. Tsubouchi, K. Yamaguchi, Y. Hayasaka, Development of an Advanced Microturbine System Using Humid Air Turbine Cycle, ASME Conference Proceedings, 2004 (2004) 167-174.

[19] K. Mochizuki, S. Shibata, U. Inoue, T. Tsuchiya, H. Sotouchi, M. Okamoto, New Concept of a Micro Gas Turbine Based Co-Generation Package for Performance Improvement in Practical Use, ASME Conference Proceedings, 2005 (2005) 1305-1310.

[20] J. Parente, A. Traverso, A.F. Massardo, Micro Humid Air Cycle: Part A – Thermodynamic and Technical Aspects, ASME Conference Proceedings, 2003 (2003) 221-229.

[21] J. Parente, A. Traverso, A.F. Massardo, Micro Humid Air Cycle: Part B – Thermoeconomic Analysis, ASME Conference Proceedings, 2003 (2003) 231-239.

[22] S. Zhang, Y. Xiao, Steady-State Off-Design Thermodynamic Performance Analysis of a Humid Air Turbine Based on a Micro Turbine, ASME Conference Proceedings, 2006 (2006) 287-296.

[23] W. De Paepe, F. Delattin, S. Bram, J. De Ruyck, Steam injection experiments in a microturbine – A thermodynamic performance analysis, Applied Energy, 97 (2012) 569-576.

[24] W. De Paepe, F. Delattin, S. Bram, J. De ruyck, Water injection in a micro gas turbine – Assessment of the performance using a black box method Applied Energy, (2012) http://dx.doi.org/10.1016/j.apenergy.2012.1011.1006.

[25] S. Bram, J. De Ruyck, Exergy analysis and design of mixed CO2/steam gas turbine cycles, Energy Conversion and Management, 36 (1995) 845-848.

[26] S. Bram, J. De Ruyck, Exergy analysis tools for Aspen applied to evaporative cycle design, Energy Conversion and Management, 38 (1997) 1613-1624.

[27] J. De Ruyck, S. Bram, G. Allard, Humid air cycle development based on exergy analysis and composite curve theory, ASME Conference Proceedings, 1995 (1995).

[28] J. De Ruyck, S. Bram, G. Allard, REVAP® Cycle: A New Evaporative Cycle Without Saturation Tower, Journal of Engineering for Gas Turbines and Power, 119 (1997) 893-897.

[29] U. Desideri, F. Di Maria, Water recovery from HAT cycle exhaust gas: a possible solution for reducing stack temperature problems, International Journal of Energy Research, 21 (1997) 809-822.

[30] M. De Paepe, E. Dick, Technological and economical analysis of water recovery in steam injected gas turbines, Applied Thermal Engineering, 21 (2001) 135-156.

[31] N.D. Årgen, M.O. Westermark, M.A. Bartlett, T. Lindquist, First Experiments on an Evaporative Gas Turbine Pilot Power Plant: Water Circuit Chemistry and Humidification Evaluation, Journal of Engineering for Gas Turbines and Power, 124 (2002) 96-102.

[32] M.A. El-Masri, A Modified, High-Efficiency, Recuperated Gas Turbine Cycle, Journal of Engineering for Gas Turbines and Power, 110 (1988) 233-242.

[33] M. Ebrahim, A. Kawari, Pinch technology: an efficient tool for chemical-plant energy and capital-cost saving, Applied Energy, 65 (2000) 45-49.

[34] P.P. Walsh, P. Fletcher, Gas turbine performance, Blackwell Science, Oxford, 2004.

[35] W. Day, D. kendrick, B. knight, A. Bhargava, W. Sowa, M. Colket, K. Casleton, D. Maloney, HAT cycle technology development program, Advanced turbine systems annual program review meeting, East Hartford,, Connecticut, 1999.

[36] A.A. Belokon, K.M. Khritov, L.A. Klyachko, S.A. Tschepin, V.M. Zakharov, J.G. Opdyke, Prediction of Combustion Efficiency and NO_x Levels for Diffusion Flame Combustors in HAT Cycles, ASME Conference Proceedings, 2002 (2002) 791-797.

[37] F. Hermann, J. Klingmann, R. Gabrielsson, Computational and Experimental Investigation of Emissions in a Highly Humidified Premixed Flame, ASME Conference Proceedings, 2003 (2003) 819-827.